Am J Cancer Res 2020;10(8):2319-2336
www.ajcr.us /ISSN:2156-6976/ajcr0116057

Original Article

Phospholipase C-ε regulates bladder cancer cells via ATM/EXO1

Jiaxin Fan[1*], Yan Zhao[1,2*], Hongling Yuan[1], Jinxiao Yang[1], Ting Li[1], Zhenting He[1], Xiaohou Wu[3], Chunli Luo[1]

[1]Key Laboratory of Diagnostics Medicine Designated by The Ministry of Education, Chongqing Medical University, Chongqing, China; [2]Department Blood of Transfusion, Affiliated Hospital of Jining Medical University, Shandong, China; [3]Department of Urology, First Affiliated Hospital of Chongqing Medical University, Chongqing, China. [*]Equal contributors.

Received June 11, 2020; Accepted July 21, 2020; Epub August 1, 2020; Published August 15, 2020

Abstract: Whole human genome microarray was performed to identify the potential molecular mechanisms associated with phospholipase C epsilon (PLCε). Gene Ontology, Kyoto Encyclopedia of Genes, and Genomes pathway analysis revealed that differentially expressed genes were significantly enriched in DNA repair-related pathways. Gene expression of PLCε, exonuclease 1 (EXO1), and ATM serine/threonine kinase (ATM) was significantly higher in 72 bladder cancer (BCa) tissue samples than in 24 samples of adjacent nonneoplastic tissue. The protein levels of PLCε and EXO1 showed appositive correlation in clinical bladder samples. Subsequent experiments showed that PLCε expression facilitated DNA repair in BCa by regulating ATM/EXO1 signaling. Additionally, we found that microRNA-145 is an antagonist of PLCε in T24 cells by directly targeting the 3'untranslated region of PLCε mRNA. Notably, microRNA-145 overexpression significantly increased the sensitivity to cisplatin, consistent with its PLCε silencing effect in BCa cells. Taken together, these findings reveal a novel physiological role for PLCε in DNA repair-related pathways with significant implications for the understanding of BCa biology.

Keywords: Phospholipase C epsilon, bladder cancer, microRNA-145, exonuclease 1, ATM serine/threonine kinase

Introduction

As one of the most prevalent urological malignancies worldwide, bladder cancer (BCa) is the eighth leading cause of cancer mortality among men in the United States, with an increasing incidence rate in recent years [1]. For early stage BCa, the recommended treatment is surgery followed by adjuvant chemotherapy, whereas radiotherapy and chemotherapy are considered as preferred treatments for late-stage cancer [2]. Cisplatin has a wide spectrum of antitumor activity and synergistic effects with multiple anticancer drugs. It is one of the most used drugs in combination on chemotherapy. Cisplatin and cisplatin-based combination therapy is commonly used in chemotherapy for BCa; however, the development of resistance to cisplatin severely limits its curative effect. Thus, clarifying the molecular mechanisms underlying the development of chemoresistance of BCa is essential.

Phospholipase C epsilon (PLCε) is a new member of the human phospholipase C family of enzymes that catalyzes the hydrolysis of phosphatidylinositol-4, 5-bisphosphate to generate two vital second messengers, inositol 1, 4, 5-triphosphate and diacylglycerol. Therefore, PLCε plays a pivotal role in the signal transduction of multiple cellular systems. Based on its structure, PLCε was found to be associated with tumorigenesis and progression of human cancers. In a previous study, we found that PLCε expression was significantly elevated in BCa tissue samples and cell lines compared with the control group [3]. Moreover, the PLCε gene was suggested to have oncogenic roles in BCa by promoting proliferation and invasion, and inhibiting apoptosis [4-6]. Therefore, PLCε is an attractive therapeutic target for BCa, although further studies are required to elucidate the mechanisms underpinning its cancer-related functions.

MicroRNAs (miRNAs) are a subset of short, non-coding RNA molecules that regulate gene expression by binding to the 3'untranslated regions (UTR) of target mRNAs [7]. Accumulating evidence indicates that miRNAs contribute to

cancer pathogenesis, chemotherapy resistance, and tumor metastasis [8-10]. Additionally, miRNAs originating from primary tumors and detected in bodily fluids such as urine, serum, or plasma, have been extensively investigated as promising biomarkers because of their relative stability and easily attainable, noninvasive nature [11]. Thus, investigating the miRNAs involved in oncogene regulation may reveal novel diagnostic markers and anticancer therapeutic targets.

DNA lesions can activate the cellular DNA damage response (DDR), which consists of a series of sophisticated mechanisms involving the coordination of cell cycle arrest, DNA damage repair, and apoptosis [12]. Recently, an important study indicated that DDR functions as "a double-edged sword" in cancer prevention and therapy. On one hand, DDR is critical for safe guarding genomic stability; on the other hand repair of radiation- or chemotherapy-induced DNA lesions can lead to unchecked DNA replication and therapy resistance in cancer cells [13]. Thus, the sensitivity of cancer cells to chemotherapy can be increased to some extent by inhibiting DNA repair pathways. Among the DNA repair components, exonuclease 1 (EXO1) is a multifunctional nuclease involved in DNA repair, replication, mismatch repair (MMR), and double-strand break repair. Recent studies showed that targeting FOXM1/EXO1 can sensitize ovarian cancer cells to cisplatin treatment [14]. Consistent with this, deficiencies in DNA2 and EXO1, in the presence of FANCD2, effectively increased the sensitivity to cisplatin [15].

In this study, we compared the gene expression profile of PLCε knockdown and control BCa cells by microarray analysis and investigated the role of PLCε in cisplatin sensitivity by dissecting the potential association between PLCε and EXO1.

Materials and methods

Patients and specimens

A total of 72 cases of carcinoma samples and 24 cases of corresponding adjacent non-neoplastic tissue samples were gathered from patients with BCa who underwent surgical resection in the Department of Urologic Surgery, the First Affiliated Hospital of Chongqing Medical University. The histological grade and stage of BCa tumors were determined according to the UICC guidelines. Enrolled patients provided informed consent and the research protocol were approved by the Ethics Committee of Chongqing Medical University. Specimens were stored in liquid nitrogen for future use.

Whole blood samples (5 mL) were collected from patients with BCa (n = 40) and patients with bladder benign diseases (BBD) (n = 19). In addition, healthy person (n = 21) were randomly selected from medical examinations with similar gender and age distributions to the patients with BCa. Within 2 hours (h), plasma was separated by centrifugation at 3,000 rpm for 10 min at 4°C, followed by a re-centrifugation at 12,000×*g* for 5 min at 4°C to remove any residual cells or debris. Then the cell-free plasma (250 μL) was added with 750 μL MagZol LS Reagent, blended immediately, and stored at -40°C for subsequent RNA extraction.

Immunohistochemistry

The tissue specimens were fixed in 10% neutral formalin, embedded in paraffin, and sectioned at 5 mm thickness. The sections were then stained and imaged as described previously [16]. The following primary antibodies were used: polyclonal rabbit antibody against PLCε (Santa Cruz, dilution 1:50), EXO1 (Elabscience, dilution 1:100), ATM (Abcam, 1:100). A semi-quantitative scoring was used to count both staining intensity and immunoreactivity ratio of the tissue sections. We counted the number of brown-stained cells and the total number of cells in each tissue section. The immunoreactivity ratio, brown-stained cells to total number of cells ratio, was 0 (0% immunoreactive cells), 1 (1-10% immunoreactive cells), 2 (11-20% immunoreactive cells), 3 (21-30% immunoreactive cells), 4 (31-40% immunoreactive cells), 5 (41-50% immunoreactive cells), 6 (51-60% immunoreactive cells), 7 (61-70% immunoreactive cells), 8 (71-80% immunoreactive cells), 9 (81-90% immunoreactive cells), and 10 (91-100% immunoreactive cells). The final immunoreactivity score was defined as the sum of both parameters. For statistical purposes, samples with a final score of 0, 1, and 2 were considered negative, while samples with other final scores were considered positive.

Cell culture and infections

Human uroepithelial cell (SV-HUC-1) and Human BCa cell lines (T24, BIU-87) were obtained from the American Type Culture

Collection (ATCC). Cell lines were maintained in RPMI 1640 medium (Gibco, USA) containing 10% FBS with 1% penicillin/streptomycin (Life Technologies, Carlsbad CA). All cells were cultured at 37°C in a humidified incubator with 5% CO_2. PLCε-targed short hairpin (sh) RNA adenovirus (Ad-shPLCε) and the negative control adenovirus (Ad-NC) were constructed as described previously [3]. When cells reached approximately 80% confluence, they were infected with the two adenoviruses.

Lipofection of miRNA mimics

Mimics of has-miR-145 (miR-145) and the negative-control (miR-NC) were purchased from GenePharma (Shanghai, China). The sequences of miR-145 mimics and miR-NC: 5'-GUCCAGUUUUCCCAGGAAUCCCU; 5'-UUCUCCGAACGUGUCACGUTT.

RNA isolation and quantitative real-time PCR

Total RNA, including miRNA was extracted from the cells using Trizol reagent (Takara, Tokyo, Japan), and the total RNA from plasma was isolated following the manufacturer's instructions (Magen, HiPure Blood RNA Kits). The total RNA (except miRNA) was reverse transcribed into cDNA using the Prime Script RT reagent kit (Takara, Tokyo, Japan). For the real-time qPCR assay, SYBR Premix Ex TaqTM II kit (Takara, Tokyo, Japan) was used according to the manufacturer's protocols. The qRT-PCR data were normalized to the expression of β-actin (miRNA was normalized to U6) using the $2^{-\Delta\Delta CT}$ method.

RNA microarrays

RNA samples for the microarray analysis were extracted from T24 cells treated with Ad-shPLCε and Ad-HK. The microarray experiments were carried out using Agilent Whole Human Genome Microarray 4×44K (Agilent Technologies, CA, USA) at Shanghai Biochip Co, Ltd (Shanghai, China). The significant analysis of microarray (SAM) method was used to screen the genes that showed a significantly difference between the two groups, and then gene clustering was conducted. Gene Ontology (GO) and Kyoto Encyclopedia of Genes (KEGG) pathway analysis were performed online (http://www.shbio.com/) to characterize their biological functions.

Cellular protein extraction and western blotting

To extract the total protein, cells were lysed in RIPA reagent supplemented with protease inhibitor mixture. The protein of membrane and cytosol were extracted separately using the Beyotime Nuclear and Cytoplasmic Protein Extraction Kit (Beyotime, China). The protein samples (30-50 μg) were separated by SDS-PAGE, then transferred onto PVDF membranes (0.45 μm, Millipore, Germany), which were blocked with 5% skim milk for 1 h at room temperature. The blots were subsequently incubated with the primary antibody, PLCε (Santa Cruz, 1:200); ATM and p-ATM (Abcam, 1:2000); EXO1 (Elabscience, 1:200); γ-H2AX (abcam, 1:1000); cyclinD1, c-myc, PCNA, caspase-3, caspase-9, Bax, Bcl-2, and H3 (bimake, 1:1000); β-actin (Zhongshan, 1:1000). The following day, the blots were incubated with an appropriate secondary antibody for 1 h at room temperature. Finally, the protein was visualized with a chemiluminescence (ECL) reagent (Millipore, USA) and analyzed with the Quantity One imaging software.

Cell viability

Cell viability was analyzed using the cell counting kit-8 (CCK-8) (Sigma-Aldrich Corp). Cells (5×10^3) were plated on a 96-well plate in 100 μL completed medium, and subjected to the indicate treatments. After culturing for 24, 48, and 72 h, 20 μL of CCK-8 (5 mg/mL) was added to each well, and the cells were then incubated for an additional 1 h. The plates were then shaken on a rotator for 10 min. Finally, the absorbance value was determined at 450 nm. The CCK-8 assays were repeated five times.

Flow cytometry assay

Cell cycle distribution and apoptosis were analyzed using flow cytometry (FCM). The quantification of apoptosis was achieved by Propidium Iodide (PI) and Annexin V staining (San Diego, CA) following the manufacturer's protocol. Briefly, cells (1×10^5) were plated into a 6-well plate overnight and treated as indicated. The cells were then harvested, separated by centrifugation and washed with cold PBS twice, followed by incubation with the stain. The stained cells were quantified by flow cytometry. The data were analyzed using FACS can cytometer Cell Quest software. For cell cycle assay, after

indicated treatments, cells were collected and fixed with 75% ethanol overnight at 4°C. The cells were then stained with PI staining solution (50 μg/mL propidium iodide, 100 μg/mL RNase, and 0.05% Triton-X) for 30 min. The DNA content of the PI-stained cells was determined by a flow cytometry.

Immunofluorescence

T24 and BIU-87 cells (3×10^4) were grown on sterile cover slips, washed twice with PBS, fixed in methyl alcohol for 15 min, permeabilized with 0.1% Triton X-100 for 15 min and blocked with 5% goat serum for 30 min at 37°C. Cells were then incubated overnight at 4°C with the primary anti p-ATM (Abcam, 1:500).

Plasmid construction and luciferase reporter assay

The 3'UTR of human PLCε gene containing the predicated target sites for miR-145, was chemically synthesized and cloned into an XbaI site of the pGL3-Basic vector (Promega, USA). The corresponding control plasmid was generated by cloning with the mutated binding sites. T24 cells were seeded in 24-well plates (3×10^4 cells per well) and were co-transfected with miR-145 mimics or the negative control and wt-PLCε-3'UTR (500 ng/well) or mt-PLCε-3'UTR (500 ng/well) luciferase plasmids. After 48 h cells were harvested and luciferase activities were determined by a Dual-luciferase Reporter Assay System (Promega, USA) according to the manufacturer's instructions.

We constructed three knock-down sequences and a negative control in the company (Gene Pharma Company, China). The knockdown effect has been verified in the previous stage [17], and then the adenovirus sequence chosen in the study are shown in the following: Ad-shPLCε-F, GGTTCTCTCCTAGAAGCAACC; Ad-shPLCε-R, CCAAGAGAGGATCTTCGTTGG. Ad-shNC-F, TTCTCCGAACGTGTCACGT; Ad-shNC-R, AAGAGGCTTGCACAGTGCA.

EXO1 human tagged ORF clone vector (RC200547), pCMV6-Entry vevtor (PS10001), vector-sh-EXO1#1 (TR304725) and vector-sh-NC (TR20003) were purchased from OriGene Technologies. Vector-sh-EXO1#2 (sc-44880-SH) was purchased from Santa Cruz Biotechnology.

Statistical analysis

Experiments were repeated at least three times and presented as the mean ± SD. Statistical comparisons were conducted using the Student's *t*-test (two groups) or one-way ANOVA analysis (more than two groups) using SPSS software (Version 17.0). Correlation between variables was determined by Pearson correlation analysis. The level of statistical significance is represented by the following: *P < 0.05; **P < 0.01; and ***P < 0.001.

Results

Prognostic significance of PLCε and EXO1 expression in BCa

Analysis of the Sanchez-Carbayo bladder dataset [18] revealed high expression of PLCε in BCa tumors (**Figure 1A**; P < 0.05). To investigate the molecular mechanisms regulated by PLCε in BCa, we compared gene expression patterns between T24 cells silenced for PLCε expression by Ad-shPLCε and T24 cells treated with Ad-NC by microarray analysis. The results indicated that PLCε mainly participated in p53, MMR, and other classical pathways (**Figure 1B**). GO enrichment analysis demonstrated that differentially expressed genes (DEGs) about MMR were associated with the following functions: cellular response to DNA damage stimulus, DNA recombination, DNA repair, and DNA metabolic process (**Figure 1C**). In addition, a two-dimensional hierarchical clustering heatmap showed the list of significant DEGs (**Figure 1D**; P < 0.05), from which four were selected to validate the microarray data by qRT-PCR. The results showed that *EXO1*, *LIG1*, and *POLD1* genes were significantly downregulated in PLCε knockdown cells, consistent with the microarray data (**Figure 1E**, **1F**). Data of 423 human bladder samples from TCGA showed that EXO1 expression in BCa specimens was significantly higher than in their non-tumor counterparts (**Figure 1G**).

Increased expression of EXO1 and ATM is associated with elevated expression of PLCε in BCa

ATM is a pivotal protein for regulating DDR, and initiating the activation of cell cycle checkpoints and DNA repair by phosphorylating multiple targets, including EXO1 and γ-H2AX [19, 20]. Here,

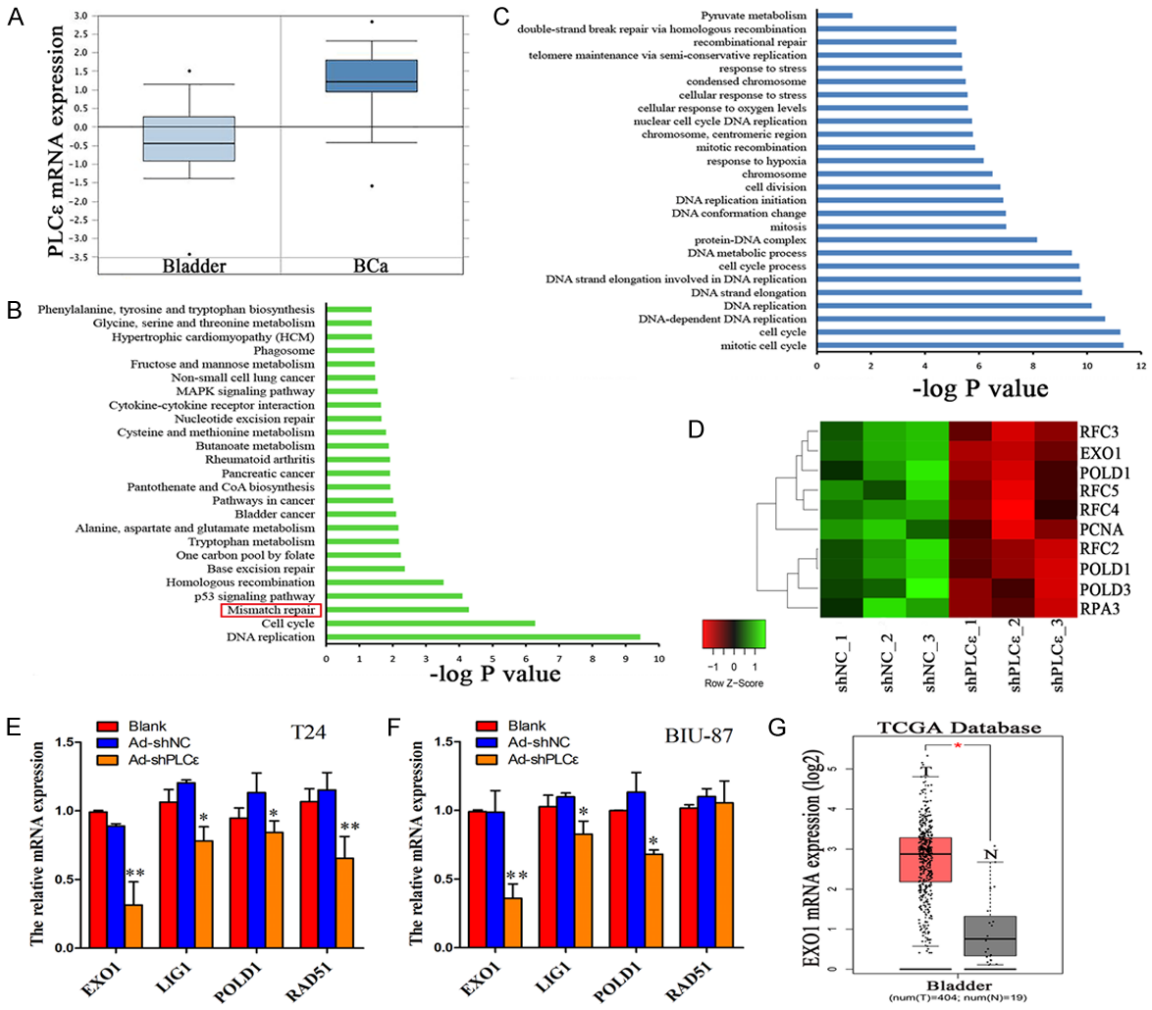

Figure 1. Gene expression profile in PLCε-silenced T24 cells and verification of selected DEGs. (A) RNA-seq mRNA expression data from Sanchez-Carbayo bladder dataset was used to compare PLCε expression between in BCa tumors (BCa) and normal bladder tissue (Bladder). (B) KEGG pathway enrichment analysis for the DEGs (> two-fold change and $P < 0.05$), the vertical axis was the pathway category, and the horizontal axis was the enrichment of pathways. (C) The significant GO category for indicated genes of mismatch repair between Ad-shPLCε and Ad-NC groups, the vertical axis was the GO terms, and the horizontal axis was the enrichment of GO, *P* value < 0.01 was used as a threshold to select significant GO categories. (D) Hierarchical clustering analysis of DEGs involved in DNA damage repair pathways. High expression levels are shown in green and low levels in red. (E, F) Detection gene levels of 4 selected DEGs by q-PCR in T24 and BIU-87 cells. The q-PCR data were normalized to the expression of β-actin (G) RNA-seq mRNA expression data from the TCGA to compare EXO1 expression between in BCa tumors (T) and their non-tumor counterparts (N). $*P \leq 0.05$, $**P \leq 0.01$, AND $***P < 0.001$.

we showed that high levels of *EXO1* and *ATM* mRNA were associated with shorter survival of patients with BCa, based on data from TCGA (**Figure 2A**, **2B**). We tested 72 samples of BCa and 24 samples of adjacent nonneoplastic (BN) tissue for the presence of PLCε, EXO1, and ATM proteins. Immunohistochemistry (IHC) analysis showed that approximately 76.39% (55/72) of the BCa samples were positive for PLCε, 79.17% (57/72) were positive for EXO1, and 87.5% (63/72) were positive for ATM (**Figure 2C**). Furthermore, Pearson's correlation analysis of IHC results confirmed a positive correlation between PLCε and EXO1 expression (**Figure 2G**; $r = 0.4376$, $P < 0.001$) and between EXO1 and ATM expression in all bladder tissues (**Figure 2H**; $r = 0.6445$, $P < 0.001$). Further statistical analysis showed that PLCε and ATM expression levels were associated with the histologic stage and grade of tumors, whereas EXO1 expression was associated only with histologic grade (**Table 1**; $P < 0.01$).

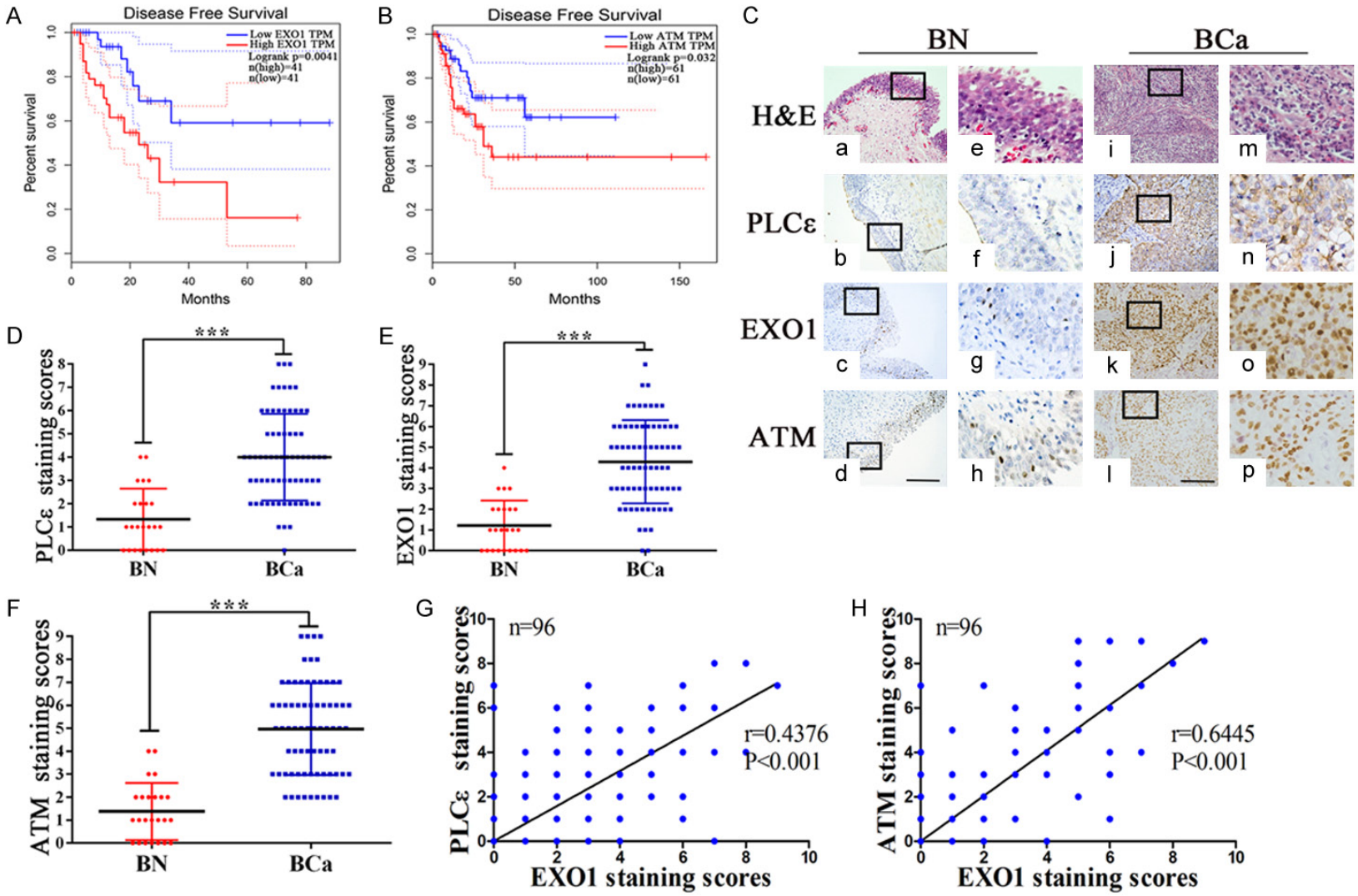

Figure 2. High expression levels of PLCε and EXO1 in BCa tissues. (A, B) Disease free survival curves of BCa patients according to EXO1 and ATM mRNA levels in TCGA. (C) Representative haematoxyl in and eosin (H&E) staining and IHC staining in 72 BCa tissue samples and 24 corresponding adjacent non-neoplastic (BN) samples. Magnification × 200. Bars = 150 μm. H&E staining of bladder tissues were showed (a and i). Representative IHC staining of different staining intensities used as criteria in staining scoring: none staining was observed in BN (b-d), positive staining in BCa (j-l). PLCε localized in cytoplasm. EXO1 and ATM protein localized in nucleus. Images in the frame of (a-d and i-l) were enlarged to (e-h and m-p). (D-F) Average staining scores for PLCε, EXO1, and ATM expression in bladder tissues. (G, H) The correlation with PLCε and EXO1 expression and EXO1 and ATM expression in bladder tissues samples was analyzed by Pearson analysis. $*P \leq 0.05$, $**P \leq 0.01$, and $***P < 0.001$.

Table 1. Correlation between PLCε, EXO1 and ATM expressions and the corresponding clinicopathological parameter in BCa patients

Variable	No. (%)	PLCε		EXO1		ATM	
		Positive	*P* value	Positive	*P* value	Positive	*P* value
Total	72 (100)	55 (76.39)		57 (79.17)		63 (87.50)	
Gender							
Male	46 (80.56)	36 (45.83)	0.412	36 (50.00)	0.527	44 (61.11)	0.388
Female	26 (19.44)	19 (30.56)		21 (29.17)		19 (26.39)	
Age (years)							
< 60	23 (31.94)	19 (26.39)	0.295	19 (26.39)	0.437	20 (27.78)	0.599
≥ 60	49 (68.06)	36 (50.00)		38 (52.78)		43 (59.72)	
Histologicstage							
Ta-T1	28 (61.11)	14 (19.44)	0.000*	24 (33.33)	0.216	21 (29.17)	0.015*
T2-T4	44 (38.89)	41 (56.94)		33 (45.83)		42 (58.33)	
Histologic grade							
Low grade	25 (34.72)	11 (15.28)	0.000*	15 (20.83)	0.005*	18 (25.00)	0.007*
High grade	47 (65.27)	44 (61.11)		42 (58.33)		45 (62.50)	
Occurrence							
Primary	61 (84.72)	45 (62.50)	0.204	49 (68.05)	0.412	53 (73.61)	0.584
Recurrence	11 (15.28)	10 (13.89)		8 (11.11)		10 (13.89)	

*Statistically significant.

Western blot analysis of 24 bladder carcinoma and BN samples showed a significant increase in PLCε and EXO1 expression in BCa compared with BN tissues (**Figure 3A-E**). Additionally, there was a positive correlation between PLCε and EXO1protein expression in all bladder tissues (**Figure 3F**).

PLCε is associated with EXO1-mediated regulation of cell cycle, proliferation, and apoptosis

We quantified PLCε and EXO1 expression in the T24, BIU-87, and SV-HUC-1 cell lines by western blotting and qRT-PCR, respectively. The results showed that PLCε and EXO1 were aberrantly expressed in T24 and BIU-87 cells compared to in SV-HUC-1 cells (**Figure 3G-I**; $P < 0.05$).

To specifically silence PLCε, BCa cells were infected with Ad-shPLCε, which markedly reduced PLCε protein levels (**Figure 4A**). Stable knockdown of PLCε was accompanied by lower expression of EXO1, cell cycle- (cyclinD1), cell proliferation-associated proteins (c-Myc, PCNA), and BCL2; in contrast, expression of apoptosis-related proteins (caspase 3, caspase 9, and BAX) was increased (**Figure 4B**).

Based on these findings, we assessed the cell cycle, proliferation, and apoptosis of tumor cells by flow cytometry and clone formation analysis. The results showed that stable knockdown of PLCε inhibited cell proliferation by inducing G1 phase arrest and apoptosis (**Figure 4A-H**). We then performed a CCK-8 assay to detect the cisplatin sensitivity in T24 and BIU-87 cells under different treatments. The data revealed that cisplatin sensitivity was significantly decreased in both cell lines compared to in SV-HUC-1 cells (**Figure 4I**). Moreover, PLCε depletion increased cisplatin sensitivity in T24 and BIU-87 cells (**Figure 4J**, **4K**). Based on these results, PLCε may be a regulator of BCa cell physiology through its effects in EXO1.

To test this hypothesis, we attempted to silence *EXO1* in BCa cells using two different shRNA vectors (vector-sh-EXO1#1 and vector-sh-EXO1#2). We confirmed that vector-sh-EXO1#2 effectively downregulated EXO1 (**Figure 5A**). Knockdown resulted in lower expression of cyclinD1, c-Myc, PCNA, and BCL2, whereas it increased the expression of caspase 3, caspase 9, and BAX (**Figure 5B**). Western blotting, flow cytometry and clone formation analysis showed that overexpression of EXO1 rescued Ad-shPLCε-transfected BCa cells from the effects of PLCε silencing, normalizing cell proliferation and apoptosis (**Figures 4E-H**, **5C**, **5D**). Together, these data support that the PLCε/EXO1 axis promotes cell proliferation and sup-

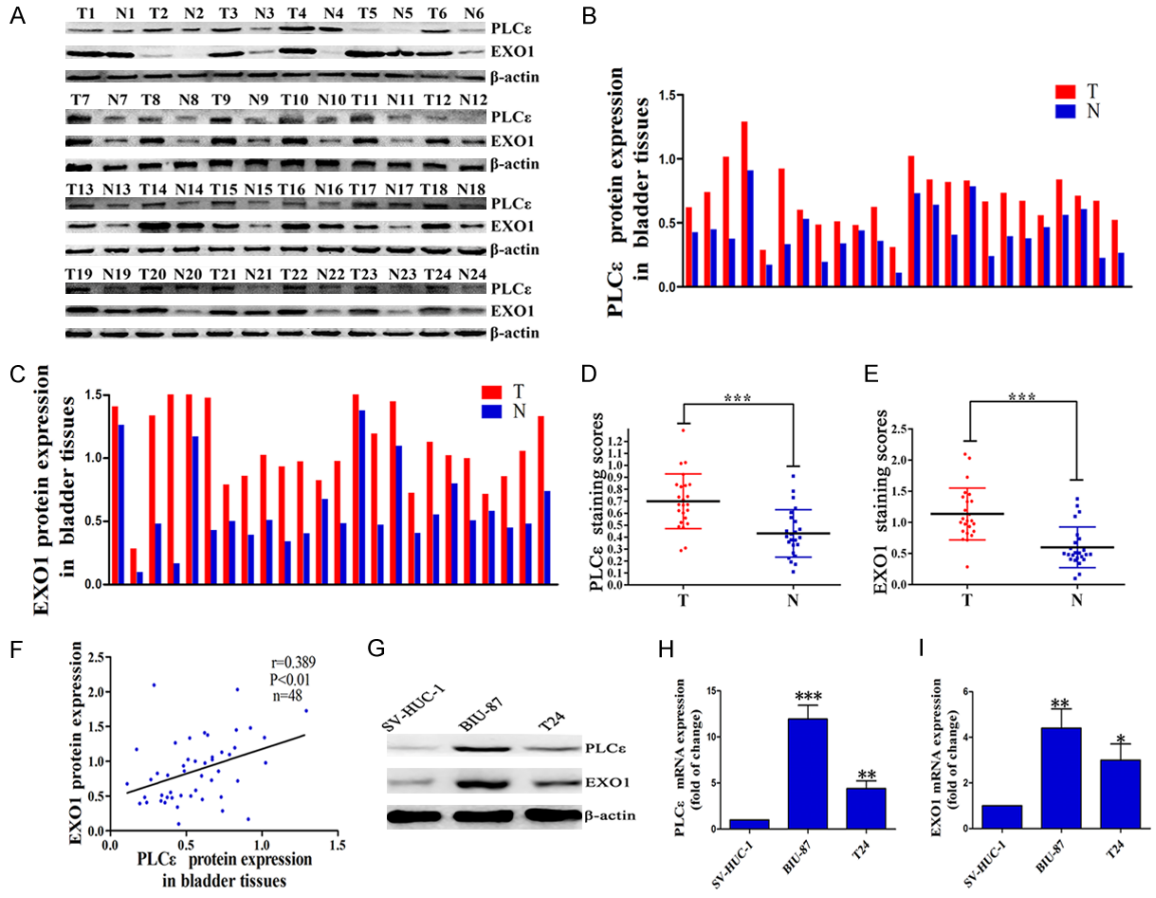

Figure 3. A association between PLCε and EXO1 expression in BCa patients. A. PLCε and EXO1 protein expression in 24 BCa tissue samples (T) and 24 BN samples (N) were assayed by western blotting analysis. B, C. PLCε and EXO1 protein expression in tissues were quantified as mean optical density by Image J software. D, E. PLCε and EXO1 protein expression in tissues were assayed by Statistical analysis. F. Correlation curve of PLCε protein versus corresponding EXO1 by Statistical analysis. G. Western blotting analysis detected the expression of PLCε and EXO1 in two human BCa cell lines and SV-HUC-1 cells. H, I. Detection of PLCε and EXO1 by qPCR. $*P \leq 0.05$, $**P \leq 0.01$, and $***P < 0.001$.

presses G1 phase arrest, apoptosis, and cisplatin sensitivity in BCa.

PLCε regulates EXO1 through nuclear translocation of p-ATM

Given the association between PLCε, EXO1, and relevant DNA repair pathways, and the correlation between ATM, PLCε, and EXO1 protein levels in BCa, we examined whether ATM participates in the PLCε/EXO1 axis.

Phosphorylation of ATM on Ser1981 (p-ATM) is a marker of ATM activation, and induces the regulation of a number of transcription factors involved in DNA repair and cell cycle check point control. To confirm the distribution of p-ATM within the nucleus, we separated nuclear and cytoplasmic cell fractions. Western blotting showed that the nuclear levels of p-ATM were notably decreased in BCa cells (**Figure 5E**). Next, we treated the cells with 13 nM of KU-55933, an ATM kinase-specific inhibitor, for 48 h and confirmed that both ATM activation and EXO1 expression were antagonized by ATM inhibition. Combined treatment with KU-55933 and PLCε depletion (Ad-shPLCε transfection) amplified such effects compared to each individual condition (**Figure 5F**). In agreement with these results, immunofluorescence staining showed that PLCε depletion markedly decreased the p-ATM signal in the nucleus and that treatment with both KU-55933 and Ad-shPLCε increased this effect versus each individual treatment (**Figure 5G**). Our results suggest that PLCε silencing downregulates the expression of EXO1 by blocking nuclear translocation of p-ATM in BCa cells.

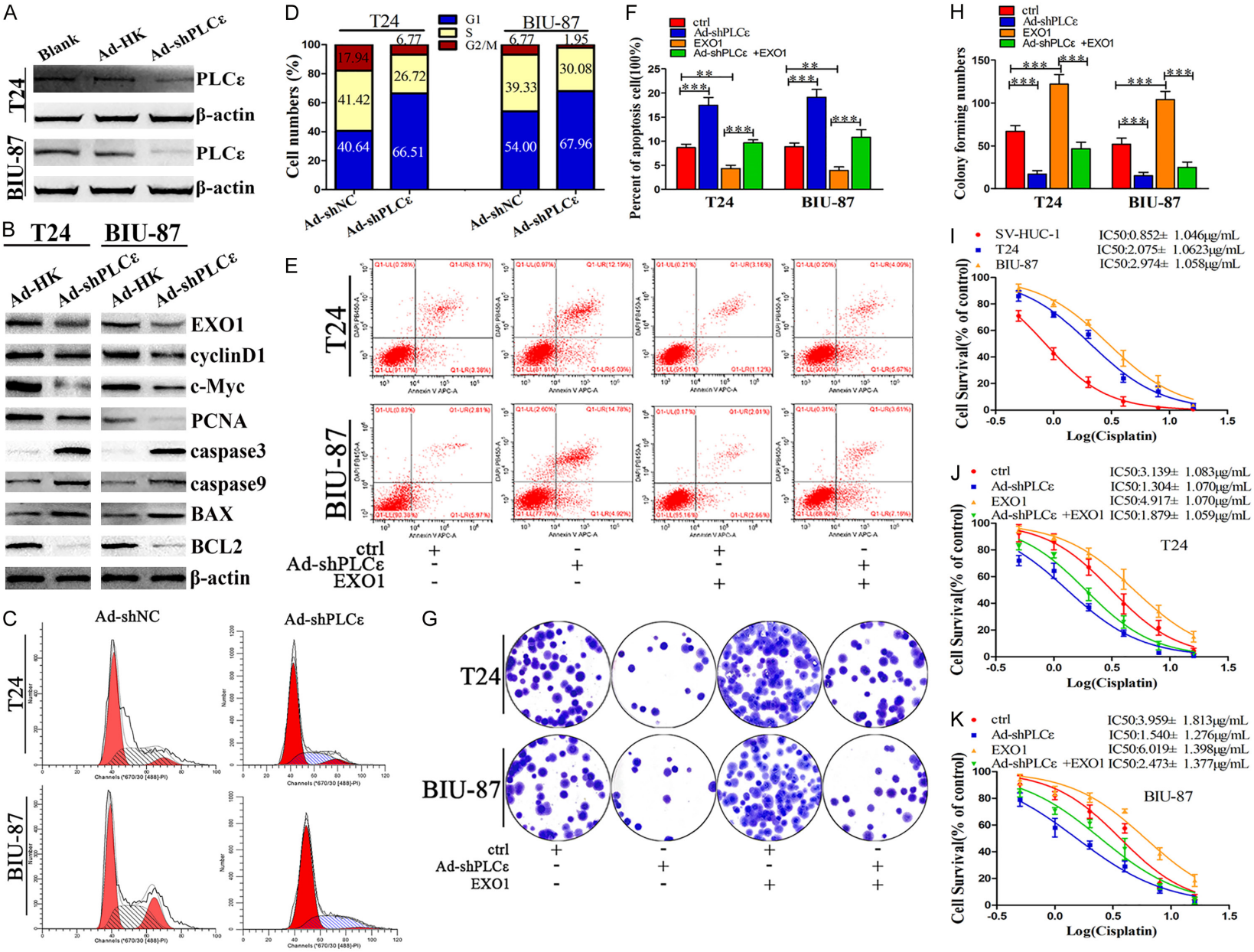
A
Blank
Ad-HK
Ad-shPLCε
T24
PLCε
β-actin
BIU-87
PLCε
β-actin
B
T24
BIU-87
Ad-HK
Ad-shPLCε
Ad-HK
Ad-shPLCε
EXO1
cyclinD1
c-Myc
PCNA
caspase3
caspase9
BAX
BCL2
β-actin
C
Ad-shNC
Ad-shPLCε
T24
BIU-87
D
T24
BIU-87
G1
S
G2/M
Cell numbers (%)
17.94
41.42
40.64
6.77
26.72
66.51
6.77
39.33
54.00
1.95
30.08
67.96
Ad-shNC
Ad-shPLCε
Ad-shNC
Ad-shPLCε
E
T24
BIU-87
ctrl
Ad-shPLCε
EXO1
F
ctrl
Ad-shPLCε
EXO1
Ad-shPLCε +EXO1
Percent of apoptosis cell(100%)
T24
BIU-87
G
T24
BIU-87
ctrl
Ad-shPLCε
EXO1
H
ctrl
Ad-shPLCε
EXO1
Ad-shPLCε +EXO1
Colony forming numbers
T24
BIU-87
I
SV-HUC-1 IC50:0.852± 1.046μg/mL
T24 IC50:2.075± 1.0623μg/mL
BIU-87 IC50:2.974± 1.058μg/mL
Cell Survival(% of control)
Log(Cisplatin)
J
ctrl IC50:3.139± 1.083μg/mL
Ad-shPLCε IC50:1.304± 1.070μg/mL
EXO1 IC50:4.917± 1.070μg/mL
Ad-shPLCε +EXO1 IC50:1.879± 1.059μg/mL
T24
Cell Survival(% of control)
Log(Cisplatin)
K
ctrl IC50:3.959± 1.813μg/mL
Ad-shPLCε IC50:1.540± 1.276μg/mL
EXO1 IC50:6.019± 1.398μg/mL
Ad-shPLCε +EXO1 IC50:2.473± 1.377μg/mL
BIU-87
Cell Survival(% of control)
Log(Cisplatin)

Figure 4. PLCε depletion inhibit cell proliferation, induce G1 phase cell cycle arrest, apoptosis and cisplatin sensitivity. A. The T24 and BIU-87 cells were infected with adenovirus sh-PLCε, western blotting were detected the expression of PLCε. B. Western blotting analysis detected the expression of EXO1, cyclinD1, c-Myc, PCNA, BCL2, caspase 3, caspase 9 and BAX. C, D. Representative flow cytometry analysis of cell cycle phase distribution after 48 h of culture, compared to blank group. E-K. The T24 and BIU-87 cells were infected with vector-EXO1 for 72 h. E, F. Representative flow cytometry analysis of cell apoptosis after 72 h of culture in Ad-shPLCε or/and EXO1 groups. G, H. Clone formation analysis was employed to test the cell proliferation in Ad-shPLCε or/and EXO1 groups. I. IC50 values were measured by CCK-8 to compare the susceptibility of the three cell lines to cisplatin. J, K. IC50 values of T24 and BIU were measured by CCK-8 Analysis in Ad-shPLCε or/and EXO1 groups. $*P \leq 0.05$, $**P \leq 0.01$, and $***P < 0.001$.

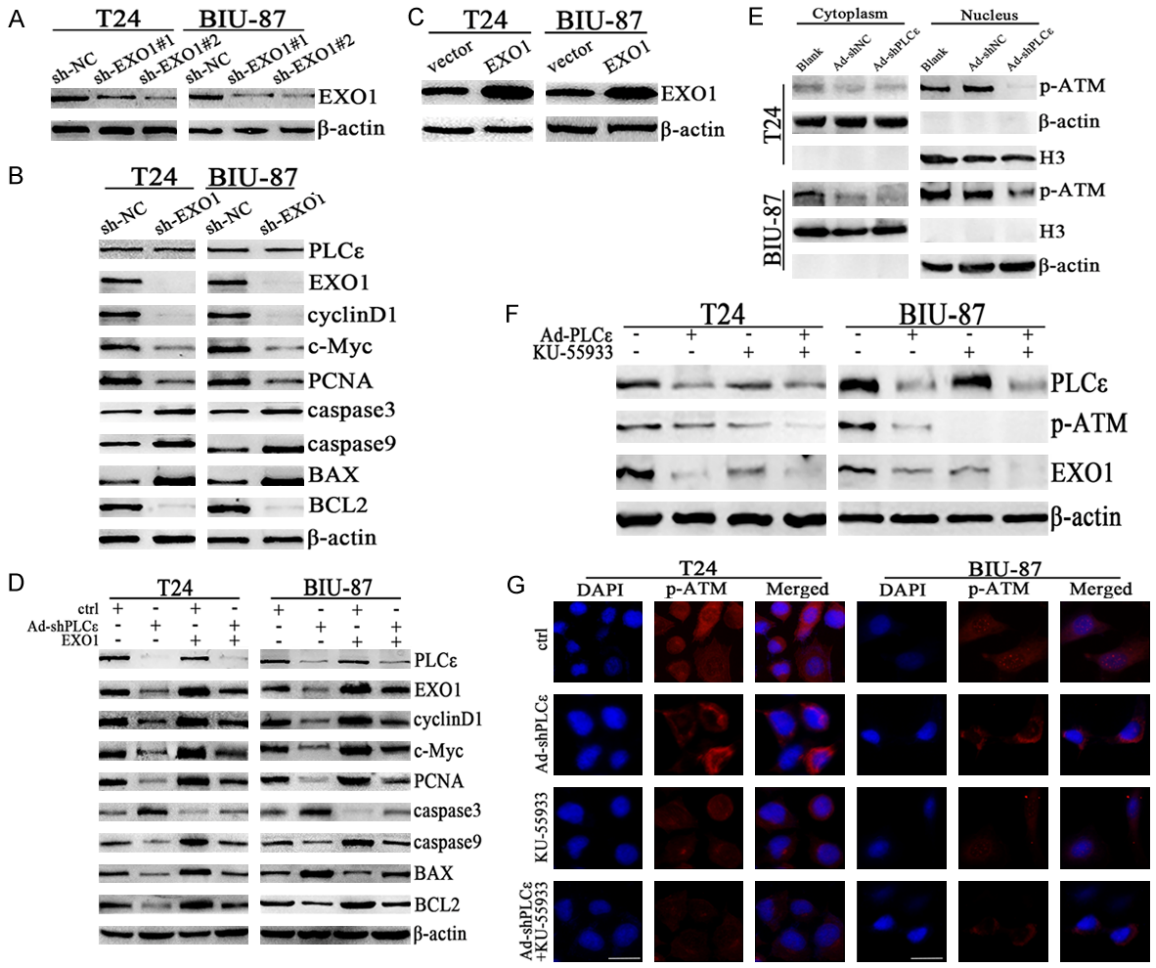

Figure 5. PLCε regulates EXO1-mediated cell cycle, proliferation and apoptosis through nuclear translocation of p-ATM. A. The BCa cells were infected with vector-shEXO1, western blotting detected the expression of EXO1. B. Western blotting analysis detected the expression of EXO1, cyclinD1, c-Myc, PCNA, BCL2, caspase 3, caspase 9, and BAX in sh-NC and sh-EXO1 groups. C. The BCa cells were infected with vector-EXO1, western blotting detected the expression of EXO1. D. Western blotting analysis detected the expression of PLCε, EXO1, cyclinD1, c-Myc, PCNA, BCL2, caspase 3, caspase 9 and BAX in sh-EXO1 groups or/and Ad-shPLCε groups. E. Detection of p-ATM expression in nuclear and cytoplasm by western blot. F. Western blotting analysis showing that Ad-shPLCε reduced EXO1 level with 13 nM KU-55933 for 48 h. G. Immunofluorescence staining analysis demonstrating that Ad-shPLCε disrupted p-ATM nuclear translocation stimulated by cisplatin. Magnification: 400×. Bars = 100 μm. $*P \leq 0.05$, $**P \leq 0.01$, and $***P < 0.001$.

PLCε depletion enhances inhibitory effect of cisplatin in BCa cell growth

Considered as one of the most reliable markers of DNA damage, γ-H2AX regulates the phosphorylation of the histone protein H2AX on Ser139. Western blotting indicated that γ-H2AX was expressed at very low levels in the control group (0 h or 0 μg/mL cisplatin), whereas it was remarkably increased following cisplatin treat-

mentin a concentration- and time-dependent manner and in parallel with elevated expression of EXO1 (**Figure 6A**, **6B**). In subsequent experiments, the cells were treated with cisplatin at 8 μg/mL for 48 h.

As shown above, PLCε depletion enhanced the sensitivity of BCa cells to cisplatin. Therefore, to investigate the synergistic effect of PLCε knockdown and cisplatin on suppressing cell proliferation, BCa cells were treated with cisplatin and/or transfected with Ad-shPLCε. Morphological changes of tumor cells exposed to cisplatin exhibited typical features of apoptosis such as irregular cell shape, visible shrinkage, and condensation (**Figure 6C**). Flow cytometry, colony formation and western blotting showed that treatment with cisplatin inhibited tumor cell proliferation and triggered apoptosis. Combining cisplatin with Ad-shPLCε transfection further enhanced this effect (**Figure 6D-I**).

Decreased levels of serum miR-145 in BCa patients and PLCε was a direct target of miR-145 in BCa cells

To explore whether miRNAs regulate PLCε expression in BCa cells, we identified the latent miRNAs targeting PLCε using the bioinformatics databases Targetscan.org, miRanda and miRbase. We used the intersection of the three databases, and then selected miRNAs based on the reported miRNA expression pattern of BCa [21-23]. The most notable candidate was miR-145, a miRNA known to function as a tumor suppressor gene in BCa. Comparison of miR-145 expression between T24, BIU and control cells by qRT-PCR showed that miR-145 was strongly expressed in SV-HUC-1 cells, but its levels were significantly lower in BIU-87 and T24 cells (**Figure 7A**). Lipofection of a miR-145 mimic strongly enhanced miR-145 expression (**Figure 7B**) and reduced that of PLCε in BCa cells (**Figure 7C**). Similar results were observed at the protein level by western blotting (**Figure 7D**), suggesting that PLCε is regulated post transcriptionally by miR-145 in T24 and BIU cells. To determine if miR-145 can bind directly to the 3'UTR of PLCε mRNA, wild-type and mutant 3'UTR sequences (**Figure 7E**) were cloned into a *luciferase* assay vector (pGL3-Basic). The recombinant plasmid was cotransfected with a miR-145 mimic or with NC (miR-NC) into T24 cells. A dual-luciferase reporter assay showed that miR-145 significantly reduced luciferase activity only when thewild-type 3'UTR was present (**Figure 7F**). Taken together, these results indicate that miR-145 direct regulates PLCε gene expression in BCa by binding to an evolutionarily conserved site in its 3'UTR.

Additionally, the CCK-8 assay showed that either miR-145 upregulation or cisplatin treatment significantly reduced the viability of BCa cells. The inhibitory effect on cell growth was further enhanced when both conditions were combined (**Figure 7G**, **7H**). Based on the relationship between miR-145 and PLCε, miR-145 executes its functions by targeting and downregulating PLCε expression. As expected, restoration of miR-145 markedly accentuated cisplatin-induced downregulation of EXO1 (**Figure 7I**). Recently, circulating miRNAs in the serum/plasma were shown to have great promise as novel, noninvasive biomarkers for cancer diagnosis and prognosis. Thus, to explore the diagnostic potential of miR-145 in BCa, the levels of serum miR-145 in 40 patients with BCa, 19 patients with BBD, and 21 healthy individuals were examined by qRT-PCR. The results indicated that the average level of miR-145 in patients with BCa was significantly lower than that in healthy individuals and patients with BBD (**Figure 7J**). Additionally, statistical analysis (**Table 2**) showed that the low-level expression of serum miR-145 was significantly associated with the histological stage ($P < 0.001$) and histological score ($P < 0.05$). These findings indicate that the circulating levels of miR-145 depletion reflect the clinicopathological characteristics of patients with BCa.

Discussion

In this study, we compared the gene expression profiles of PLCε knockdown BCa cells with control cells by microarray analysis. First, we found that PLCε was involved in EXO1-associated DNA repair pathways. Second, we confirmed that miR-145 was downregulated both in BCa cell lines and in the plasma of patients with BCa and discovered that PLCε is directly regulated by miR-145, a tumor suppressive miRNA (**Figure 8**). Importantly, by directly targeting PLCε mRNA, miR-145 leads to enhanced cisplatin sensitivity.

PLCε is a Ras effector shown to play pivotal roles in multiple cancer types [5, 17, 24-26]. Here, we first analyzed the role of PLCε on genome-wide expression of BCa and then

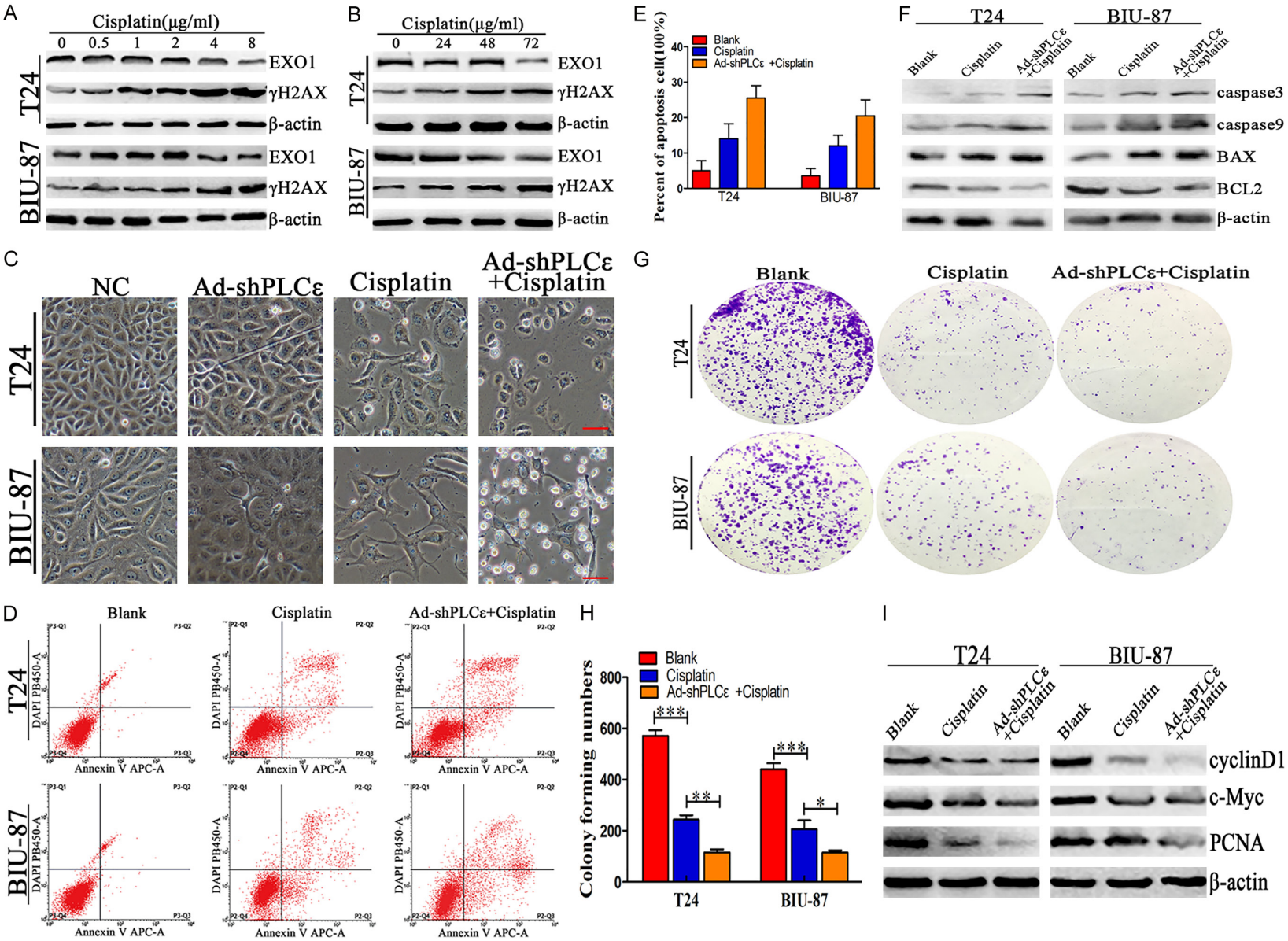

Figure 6. PLCε depletion enhanced the inhibitory effect of cisplatin on the growth of BCa cells. C-I. 8 μg/mL Cisplatin was treated in BCa cells for 48 h. A, B. Western blotting analysis showing the expressions of EXO1 and γ-H2AX stimulated by cisplatin at different concentrations (for 24 h) and different treat times (with 8 μg/mL) in BCa cells. C. Morphological change of bladder cancer cells with cisplatin or (and) Ad-shPLCε treatment. Magnification: 200×. Bars = 100 μm. D, E. Representative

flow cytometry analysis of cell cycle phase distribution after 48 h of culture, compared to blank group. F. Western blotting detected the expression of cell cycle and proliferation related proteins. G, H. Clone formation analysis was employed to test the cell proliferation of BCa cell lines after treatment with cisplatin. I. Western blotting detected the expression of cell apoptosis related proteins. *P ≤ 0.05, **P ≤ 0.01, and ***P < 0.001.

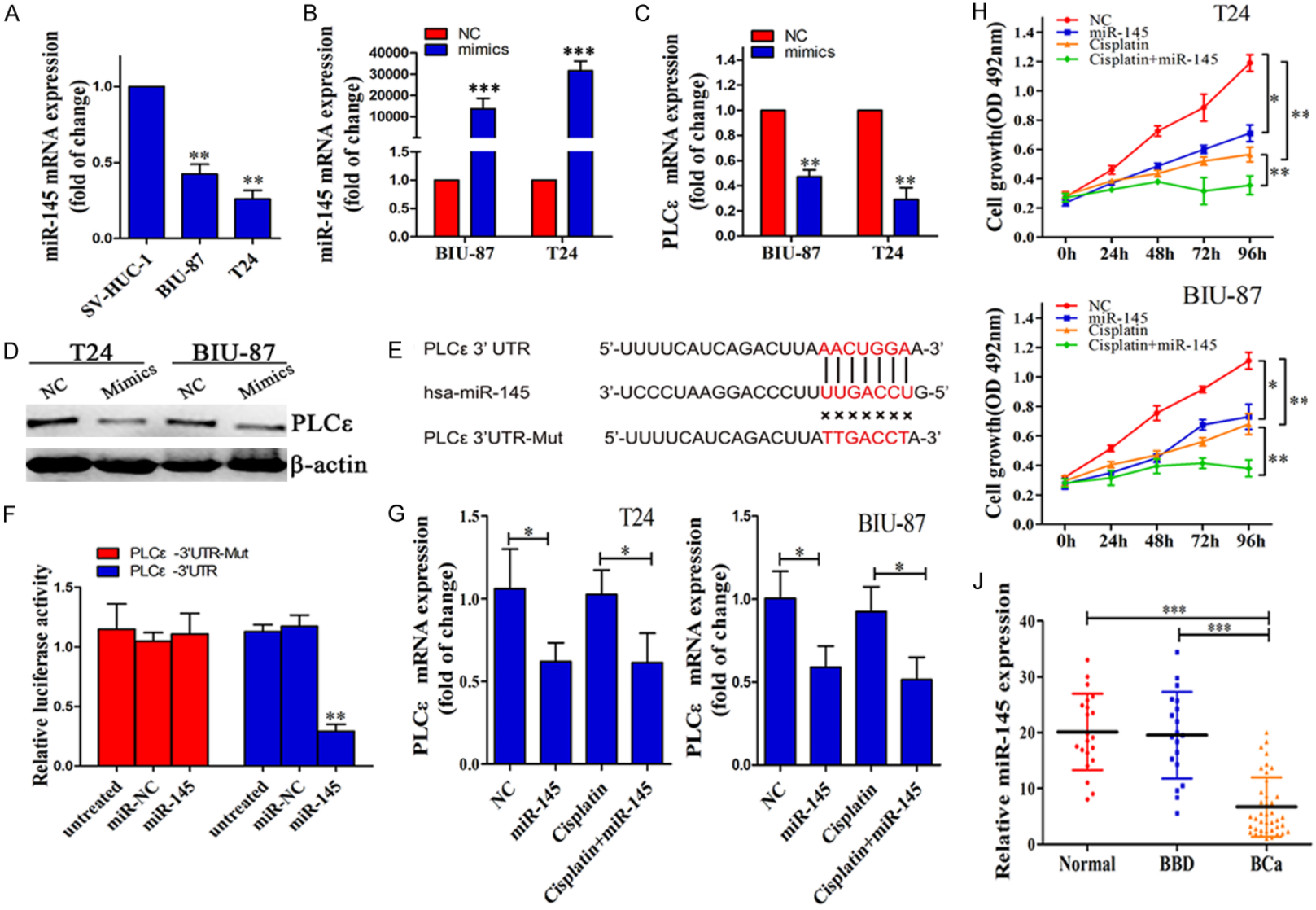

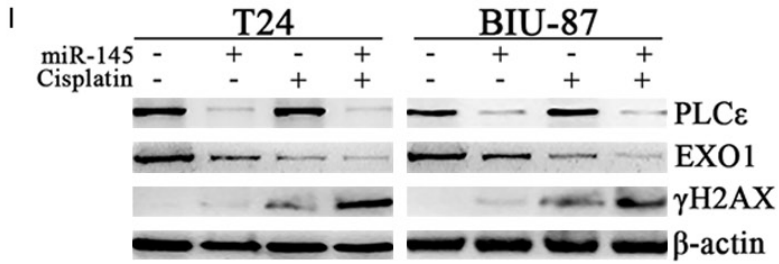

Figure 7. Decreased levels of serum miR-145 in BCa patients and PLCε was a direct target of miR-145 in BCa cells. A. Comparison of miR-145 levels in three cell lines by qPCR. vs SV-HUC-1. B. Expression levels of miR-145 in T24 and BIU cells transfected with miR-145 mimics and NC. C, D. PLCε mRNA and protein expression levels in the BCa cell lines detected by qRT-PCR and western blotting after transfection with miR-145 mimics. E. Schematic representation of the predicted miR-145 binding sites in 3'UTR of PLCε. F. Wild-type or mutant 3'UTR of PLCε gene reporter plasmid was co-transfected with miR-145mimics or NC into T24, followed by luciferase reporter assays. vs miR-NC. G. Changes of PLCε expression analysised by qPCR in BCa cells after treating with cisplatin or (and) miR-145. H, I. 8 μg/mL Cisplatin was treated in BCa cells for 48 h. H. Viability of BCa cells with cisplatin or (and) miR-145 mimics treatment detected by CCK-8. I. Western blotting analysis showing the expression of PLCε, EXO1, and γH2AX after cisplatin or (and) miR-145 mimics treatment for 48 h. J. The serum miR-145 expression in 40 patients with BCa, 19 patients with urinary benign diseases (BBD) and 21 healthy controls (Normal) were obtained by qPCR. Expression levels of miR-145 were normalized to U6. $*P \leq 0.05$, $**P \leq 0.01$, and $***P < 0.001$.

Table 2. miR-145 in BCa patients serum and clinicopathological parameters

Variable	No. (%)	miR-145 expression	*P* values
Total	40 (100)	6.68±5.19	
Gender			0.0942
Male	31 (77.50)	5.91±5.07	
Female	9 (22.50)	9.29±5.03	
Age (years)			
< 60	14 (35.00)	8.44±6.44	0.1257
≥ 60	26 (65.00)	5.72±4.19	
Histologic stage			
Ta-T1	13 (32.50)	10.8±5.88	0.0003*
T2-T4	27 (67.50)	4.69±3.49	
Histologic score			
Low grade	18 (45.00)	8.68±6.17	0.0292*
High grade	22 (55.00)	5.03±3.61	
Occurrence			
Primary	34 (85.00)	6.84±5.44	0.6335
Recurrence	6 (15.00)	5.70±3.92	

*Statistically significant.

focused on its role in the MMR pathway. PLCε is considered as an anticancer therapeutic target because of its ability to increase sensitivity to standard chemotherapy [27, 28]. As an effector of MMR, high expression levels of EXO1 were found in most BCa tissues compared with in adjacent tissues, consistent with a prior report [29]. We used patient bladder tissues to comprehensively analyze PLCε and EXO1 expression. The results indicated that high expression of PLCε and EXO1 in BCa tissues was correlated with an advanced histologic stage and grade. Moreover, a positive correlation was found between PLCε and EXO1 expression. Thus, measurement of PLCε and EXO1 expression may have diagnostic and/or prognostic value in BCa.

In this study, we downregulated PLCε expression in BCa cell lines by adenovirus-mediated knockdown. Depletion of PLCε reduced the expression of EXO1, BCL2, cell cycle- (cyclinD1) and proliferation-associated proteins (c-Myc and PCNA) and upregulated the expression of apoptosis-related proteins (caspase 3, caspase 9 and BAX). Knockdown of EXO1 using shRNA clearly showed that PLCε regulates the cell cycle, proliferation, apoptosis and cisplatin sensitivity of BCa cells by targeting EXO1.

As a DNA damage sensor, ATM kinase initiates the cellular response to DSBs [30] and activates numerous DNA repair proteins [31]. In this study, we found that PLCε silencing lowers the levels of p-ATM and its downstream target EXO1. Importantly, immunofluorescence and western blot analyses indicated that PLCε deficiency likely block p-ATM nuclear translocation. Thus, we demonstrated that ATM participates in the PLCε/EXO1 axis in BCa cells.

Cisplatin-based chemotherapy is commonly used to treat BCa, particularly for locally advanced and metastatic BCa. Cisplatin exerts cytotoxic effects by binding to DNA and inducing DSBs. These breaks can be recognized by multiple repair pathways such as nucleotide excision repair and MMR [32]. However, the therapeutic efficacy of cisplatin is often unsatisfactory because of the emergence of drug resistance. Failure to repair drug-induced DNA damage is crucial for rendering cancer cells sensitive to cytotoxic chemotherapy [33, 34]. Our data suggests that elevated PLCε may contribute to BCa high resistance to cisplatin, whereas low PLCε enhances the cytotoxic effect of cisplatin.

Given that miRNAs are considered as strong regulators of gene expression, we identified the miRNAs regulating PLCε expression using bioinformatics databases. By combining data from previous studies, we selected miRNA-145 as a potential candidate [35, 36]. Our data showed that upregulation of PLCε directly correlates with low miR-145 expression and that miR-145 binds to target sequences in the 3'UTR of PLCε mRNA. We also confirmed that overexpression of miR-145 further downregulates EXO1 induced by cisplatin. This indicates miR-145-mediated PLCε knockdown is a potential therapeutic approach for treating BCa, particularly cisplatin-resistant tumors. As circulating microRNAs are stable and readily detectable in the human serum [37, 38], they are regarded as potential diagnostic and prognostic biomarkers for various cancers [39-41]. Taken together, our results suggest that serum levels of miR-145 can mirror tumor dynamics and serve as a biomarker for monitoring of the tumor status or early detection of BCa.

Conclusion

Our study provides insight into the role of PLCε in the cell cycle, proliferation, apoptosis, and cisplatin sensitivity of BCa. We found that the effects of PLCε are mediated by ATM/EXO1 and

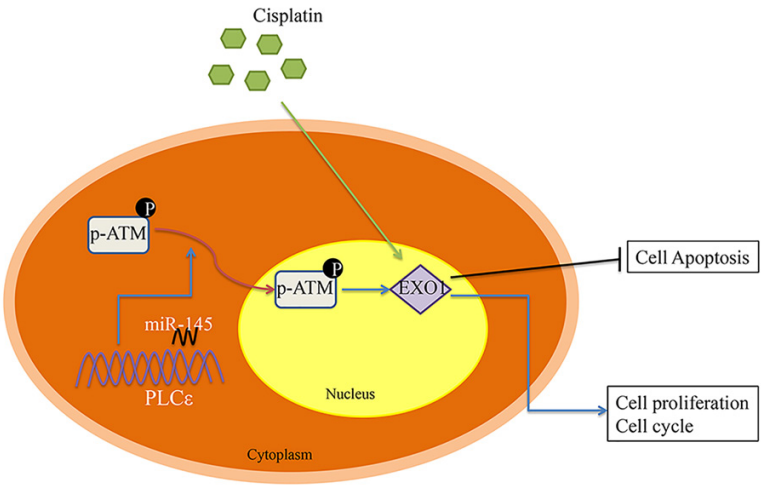

Figure 8. A mechanism for PLCε depletion-mediated cisplatin sensitivity of BCa. Schematic diagram describing the functional significance of PLCε in BCa cells. PLCε regulate EXO1 medicated-cell cycle, proliferation, apoptosis and cisplatin sensitivity through nuclear translocation of p-ATM and can be regulated by miR-145.

that PLCε expression is directly regulated by miR-145, a tumor suppressive miRNA. Overall, our results provide evidence that miR-145 is a promising biomarker or novel therapeutic target for BCa.

Acknowledgements

The authors thank the patients and their families who generously donated valuable samples. Our work was supported by grants from the National Natural Science Foundation of China (No. 81072086), and the Scientific and Technological Research Program of Chongqing Municipal Education Committee (No. KJ110-305).

Disclosure of conflict of interest

None.

Address correspondence to: Chunli Luo, Key Laboratory of Diagnostics Medicine Designated by The Ministry of Education, Chongqing Medical University, Chongqing 400016, China. E-mail: luochunli555@163.com

References

[1] Siegel RL, Miller KD and Jemal A. Cancer Statistics, 2017. CA Cancer J Clin 2017; 67: 7-30.

[2] Suer E, Hamidi N, Gokce MI, Gulpinar O, Turkolmez K, Beduk Y and Baltaci S. Significance of second transurethral resection on patient outcomes in muscle-invasive bladder cancer patients treated with bladder-preserving multimodal therapy. World J Urol 2016; 34: 847-51.

[3] Ou L, Guo Y, Luo C, Wu X, Zhao Y and Cai X. RNA interference suppressing PLCE1 gene expression decreases invasive power of human bladder cancer T24 cell line. Cancer Genet Cytogenet 2010; 200: 110-9.

[4] Cheng H, Luo C, Wu X, Zhang Y, He Y, Wu Q, Xia Y and Zhang J. shRNA targeting PLCepsilon inhibits bladder cancer cell growth in vitro and in vivo. Urology 2011; 78: 474, e7-11.

[5] Du HF, Ou LP, Yang X, Song XD, Fan YR, Tan B, Luo CL and Wu XH. A new PKCalpha/beta/TBX3/E-cadherin pathway is involved in PLCepsilon-regulated invasion and migration in human bladder cancer cells. Cell Signal 2014; 26: 580-93.

[6] Zhang Y, Yan L, Zhao Y, Ou L, Wu X and Luo C. Knockdown of phospholipase C-epsilon by short-hairpin RNA-mediated gene silencing induces apoptosis in human bladder cancer cell lines. Cancer Biother Radiopharm 2013; 28: 233-9.

[7] Ruan K, Fang X and Ouyang G. MicroRNAs: novel regulators in the hallmarks of human cancer. Cancer Lett 2009; 285: 116-26.

[8] Lv L, Li Y, Deng H, Zhang C, Pu Y, Qian L, Xiao J, Zhao W, Liu Q, Zhang D, Wang Y, Zhang H, He Y and Zhu J. MiR-193a-3p promotes the multichemoresistance of bladder cancer by targeting the HOXC9 gene. Cancer Lett 2015; 357: 105-113.

[9] Rokavec M, Öner MG, Li H, Jackstadt R, Jiang L, Lodygin D, Kaller M, Horst D, Ziegler PK, Schwitalla S, Slotta-Huspenina J, Bader FG, Greten FR and Hermeking H. IL-6R/STAT3/miR-34a feedback loop promotes EMT-mediated colorectal cancer invasion and metastasis. J Clin Invest 2014; 124: 1853-67.

[10] Yu F, Deng H, Yao H, Liu Q, Su F and Song E. Mir-30 reduction maintains self-renewal and inhibits apoptosis in breast tumor-initiating cells. Oncogene 2010; 29: 4194-204.

[11] Jiang X, Du L, Wang L, Li J, Liu Y, Zheng G, Qu A, Zhang X, Pan H, Yang Y and Wang C. Serum microRNA expression signatures identified

from genome-wide microRNA profiling serve as novel noninvasive biomarkers for diagnosis and recurrence of bladder cancer. Int J Cancer 2015; 136: 854-62.
[12] Jackson SP and Bartek J. The DNA-damage response in human biology and disease. Nature 2009; 461: 1071-8.
[13] Tian H, Gao Z, Li H, Zhang B, Wang G, Zhang Q, Pei D and Zheng J. DNA damage response--a double-edged sword in cancer prevention and cancer therapy. Cancer Lett 2015; 358: 8-16.
[14] Zhou J, Wang Y, Wang Y, Yin X, He Y, Chen L, Wang W, Liu T and Di W. FOXM1 modulates cisplatin sensitivity by regulating EXO1 in ovarian cancer. PLoS One 2014; 9: e96989.
[15] Karanja KK, Cox SW, Duxin JP, Stewart SA and Campbell JL. DNA2 and EXO1 in replication-coupled, homology-directed repair and in the interplay between HDR and the FA/BRCA network. Cell Cycle 2012; 11: 3983-96.
[16] Quan Z, He Y, Luo C, Xia Y, Zhao Y, Liu N and Wu X. Interleukin 6 induces cell proliferation of clear cell renal cell carcinoma by suppressing hepaCAM via the STAT3-dependent up-regulation of DNMT1 or DNMT3b. Cell Signal 2017; 32: 48-58.
[17] Fan J, Fan Y, Wang X, Niu L, Duan L, Yang J, Li L, Gao Y, Wu X and Luo C. PLCepsilon regulates prostate cancer mitochondrial oxidative metabolism and migration via upregulation of Twist1. J Exp Clin Cancer Res 2019; 38: 337.
[18] Sanchez-Carbayo M, Socci ND, Lozano J, Saint F and Cordon-Cardo C. Defining molecular profiles of poor outcome in patients with invasive bladder cancer using oligonucleotide microarrays. J Clin Oncol 2006; 24: 778-89.
[19] Berkovich E, Monnat RJ Jr and Kastan MB. Roles of ATM and NBS1 in chromatin structure modulation and DNA double-strand break repair. Nat Cell Biol 2007; 9: 683-90.
[20] Shiloh Y and Ziv Y. The ATM protein kinase: regulating the cellular response to genotoxic stress, and more. Nat Rev Mol Cell Biol 2013; 14: 197-210.
[21] Canturk KM, Ozdemir M, Can C, Öner S, Emre R, Aslan H, Cilingir O, Ciftci E, Celayir FM, Aldemir O, Özen M and Artan S. Investigation of key miRNAs and target genes in bladder cancer using miRNA profiling and bioinformatic tools. Mol Biol Rep 2014; 41: 8127-35.
[22] Ichimi T, Enokida H, Okuno Y, Kunimoto R, Chiyomaru T, Kawamoto K, Kawahara K, Toki K, Kawakami K, Nishiyama K, Tsujimoto G, Nakagawa M and Seki N. Identification of novel microRNA targets based on microRNA signatures in bladder cancer. Int J Cancer 2009; 125: 345-52.
[23] Ratert N, Meyer HA, Jung M, Lioudmer P, Mollenkopf HJ, Wagner I, Miller K, Kilic E, Erbersdobler A, Weikert S and Jung K. miRNA profiling identifies candidate mirnas for bladder cancer diagnosis and clinical outcome. J Mol Diagn 2013; 15: 695-705.
[24] Wang Y, Wu X, Ou L, Yang X, Wang X, Tang M, Chen E and Luo C. PLCepsilon knockdown inhibits prostate cancer cell proliferation via suppression of Notch signalling and nuclear translocation of the androgen receptor. Cancer Lett 2015; 362: 61-9.
[25] Nash CA, Wei W, Irannejad R and Smrcka AV. Golgi localized beta1-adrenergic receptors stimulate Golgi PI4P hydrolysis by PLCepsilon to regulate cardiac hypertrophy. Elife 2019; 8: e48167.
[26] Du HF, Ou LP, Song XD, Fan YR, Yang X, Tan B, Quan Z, Luo CL and Wu XH. Nuclear factor-kappaB signaling pathway is involved in phospholipase Cepsilon-regulated proliferation in human renal cell carcinoma cells. Mol Cell Biochem 2014; 389: 265-75.
[27] Begum R and Martin SA. Targeting mismatch repair defects: a novel strategy for personalized cancer treatment. DNA Repair (Amst) 2016; 38: 135-139.
[28] Gavande NS, VanderVere-Carozza PS, Hinshaw HD, Jalal SI, Sears CR, Pawelczak KS and Turchi JJ. DNA repair targeted therapy: the past or future of cancer treatment? Pharmacol Ther 2016; 160: 65-83.
[29] Muthuswami M, Ramesh V, Banerjee S, Viveka Thangaraj S, Periasamy J, Bhaskar Rao D, Barnabas GD, Raghavan S and Ganesan K. Breast tumors with elevated expression of 1q candidate genes confer poor clinical outcome and sensitivity to Ras/PI3K inhibition. PLoS One 2013; 8: e77553.
[30] Técher H, Koundrioukoff S, Carignon S, Wilhelm T, Millot GA, Lopez BS, Brison O and Debatisse M. Signaling from Mus81-Eme2-dependent DNA damage elicited by Chk1 deficiency modulates replication fork speed and origin usage. Cell Rep 2016; 14: 1114-1127.
[31] Falck J, Coates J and Jackson SP. Conserved modes of recruitment of ATM, ATR and DNA-PKcs to sites of DNA damage. Nature 2005; 434: 605-11.
[32] Dasari S and Tchounwou PB. Cisplatin in cancer therapy: molecular mechanisms of action. Eur J Pharmacol 2014; 740: 364-78.
[33] Galluzzi L, Senovilla L, Vitale I, Michels J, Martins I, Kepp O, Castedo M and Kroemer G. Molecular mechanisms of cisplatin resistance. Oncogene 2012; 31: 1869-83.
[34] Plimack ER, Dunbrack RL, Brennan TA, Andrake MD, Zhou Y, Serebriiskii IG, Slifker M, Alpaugh K, Dulaimi E, Palma N, Hoffman-Censits J, Bilusic M, Wong YN, Kutikov A, Viterbo R, Greenberg RE, Chen DY, Lallas CD,

Trabulsi EJ, Yelensky R, McConkey DJ, Miller VA, Golemis EA and Ross EA. Defects in DNA repair genes predict response to neoadjuvant cisplatin-based chemotherapy in muscle-invasive bladder cancer. Eur Urol 2015; 68: 959-67.

[35] Xu Q, Liu LZ, Qian X, Chen Q, Jiang Y, Li D, Lai L and Jiang BH. MiR-145 directly targets p70S6K1 in cancer cells to inhibit tumor growth and angiogenesis. Nucleic Acids Res 2012; 40: 761-74.

[36] Yoshino H, Seki N, Itesako T, Chiyomaru T, Nakagawa M and Enokida H. Aberrant expression of microRNAs in bladder cancer. Nat Rev Urol 2013; 10: 396-404.

[37] Mitchell PS, Parkin RK, Kroh EM, Fritz BR, Wyman SK, Pogosova-Agadjanyan EL, Peterson A, Noteboom J, O'Briant KC, Allen A, Lin DW, Urban N, Drescher CW, Knudsen BS, Stirewalt DL, Gentleman R, Vessella RL, Nelson PS, Martin DB and Tewari M. Circulating microRNAs as stable blood-based markers for cancer detection. Proc Natl Acad Sci U S A 2008; 105: 10513-8.

[38] Yun SJ, Jeong P, Kim WT, Kim TH, Lee YS, Song PH, Choi YH, Kim IY, Moon SK and Kim WJ. Cell-free microRNAs in urine as diagnostic and prognostic biomarkers of bladder cancer. Int J Oncol 2012; 41: 1871-8.

[39] Chan M, Liaw CS, Ji SM, Tan HH, Wong CY, Thike AA, Tan PH, Ho GH and Lee AS. Identification of circulating microRNA signatures for breast cancer detection. Clin Cancer Res 2013; 19: 4477-87.

[40] Haldrup C, Kosaka N, Ochiya T, Borre M, Høyer S, Orntoft TF and Sorensen KD. Profiling of circulating microRNAs for prostate cancer biomarker discovery. Drug Deliv Transl Res 2014; 4: 19-30.

[41] Zhang Y, Zhang D, Wang F, Xu D, Guo Y and Cui W. Serum miRNAs panel (miR-16-2*, miR-195, miR-2861, miR-497) as novel non-invasive biomarkers for detection of cervical cancer. Sci Rep 2015; 5: 17942.